

## Electronic Supporting Information for

# **Tin-oxychalcogenide supertetrahedral clusters maintained in an MTN zeolite-analog arrangement by Coulombic interactions**

Ming-Bu Luo,<sup>a,b</sup> Shan-Lin Huang,<sup>a,b</sup> Heng-Dong Lai,<sup>a</sup> Jian Zhang<sup>\*,a</sup> and Qipu Lin<sup>\*,a</sup>

<sup>a</sup>*State Key Laboratory of Structural Chemistry Fujian Institute of Research on the  
Structure of Matter, Chinese Academy of Sciences, Fuzhou, Fujian 350002, China*

<sup>b</sup>*University of Chinese Academy of Sciences, Beijing 100049, China*

\*Corresponding Author: Email: [zhj@fjirsm.ac.cn](mailto:zhj@fjirsm.ac.cn); [linqipu@fjirsm.ac.cn](mailto:linqipu@fjirsm.ac.cn)

## **Table of Contents**

**Section S1:** General Methods

**Section S2:** Synthetic Procedures

**Section S3:** Crystallographic Data

**Section S4:** Fourier-Transform Infrared (FT–IR) Spectroscopy and  
Thermogravimetric Analysis (TGA)

**Section S5:** Scanning Electron Microscopy (SEM) and X-ray Energy  
Dispersive Spectroscopy (EDS)

**Section S6:** Electrospray Ionization Mass Spectrometry (ESI–MS)

**Section S7:** Gas Sorption (BET)

**Section S8:** Photoluminescence (PL)

**Section S9:** Proton Conduction

**Section S10:** References

## Section S1: General Methods

**Chemicals:** *n*-Butyltin trichloride (*n*-butylSnCl<sub>3</sub>, 98%, liquid), *n*-butyl alcohol (99.5%, liquid), 1,5-Diazabicyclo[4.3.0]non-5-ene (DBN, 99%, liquid), thiourea (99%, solid), SeO<sub>2</sub> (99%, solid), 1,4-diaminobutane (DBA, 98%, liquid), 1-butyl-2,3-dimethylimidazolium chloride ([BMMIm]Cl, 99%, solid), Dimethyl sulfoxide (DMSO, 99.5%, liquid) were all used as supplied without further purification.

**Instrumentation:** Energy dispersive spectroscopy (EDS) analysis was performed on scanning electron microscope (SEM) equipped with Oxford INCA system. Elemental analysis (EA) was carried out on a Vario EL-Cube. Inductively coupled plasma optical emission spectroscopy (ICP–OES) was performed on an Ultima-2 spectrometer. The powder X-ray diffraction (PXRD) data of the samples were collected on a Rigaku Mini Flex II diffractometer using Cu K $\alpha$  radiation ( $\lambda = 1.54056 \text{ \AA}$ ) under ambient conditions. The UV–Vis diffuse reflection spectroscopy (DRS) data were recorded at room temperature using a powder sample with BaSO<sub>4</sub> as a standard (100% reflectance) on a PerkinElmer Lambda-950 UV spectrophotometer and scanned at 250–800 nm. Thermo gravimetric analysis (TGA) was carried out on a Mettler Toledo TGA/SDTA 851e analyzer in air atmosphere with a heating rate of 10 °C min<sup>−1</sup> from 25 to 800 °C. Fourier transform infrared (FT–IR) spectra were acquired using KBr pellets on a Nicolet Magna 750 FT–IR spectrometer over a range 400–4000 cm<sup>−1</sup>. The gas adsorption measurements were performed on a Micromeritics ASAP 2020 surface area and pore size analyzer. Electrospray ionization mass spectrometry (ESI–MS) data were collected on a DECA- 30000 LCQ Deca XP instrument. Fluorescence was recorded on an Edinburgh FLS980 fluorescent photometer.

**Single Crystal Characterization:** The single crystal X-ray diffraction measurement was performed on ROD, Synergy Custom system, HyPix diffractometer with micro-focus metaljet K $\alpha$  ( $\lambda = 1.34050 \text{ \AA}$ ) radiation at 100 K. The structure was solved by direct method and refined by full-matrix least-squares on  $F^2$  using the olex2.<sup>1</sup> All the non-hydrogen atoms are refined anisotropically. Contributions to scattering due to disordered solvent molecules were removed using the SQUEEZE routine of PLATON.<sup>2</sup>

Structures were then refined again using the data generated.

**Photoelectric Response:** Fluorine-doped tin oxide (FTO) glasses were cleaned by sonication in the acetone for half an hour and then dried at 60 °C over night in an oven. Then the dry and clean FTO glasses were used as the working electrodes. 5 mg sample was dispersed in the 0.5 ml solvent (T3-SnOS-MTN in DMF and T3-SnOSe-MTN in CH<sub>3</sub>OH) and sonicated for 1 hour to get slurry. The conductive tape was used to adhere to part of FTO glasses to leave a circle with an area of 0.25 cm<sup>2</sup> for the slurry and then dried at room temperature naturally. The photocurrent measurements were performed in the cell equipped with three electrodes in the presence of 0.2 M Na<sub>2</sub>SO<sub>4</sub> solution. A 300W Xe lamp (Beijing perfectlight, PLS-SXE300c) with a 420 nm cut-off filter was prepared for the photocurrent tests.

## Section S2: Synthetic Procedures

**Synthesis of T3-SnOS-MTN.** *n*-butylSnCl<sub>3</sub> (0.1 mL), thiourea (3 mmol), DBN (1 mL), *n*-butyl alcohol (3 mL), were mixed in a 23-mL Teflon-lined stainless autoclave and stirred for 10 minutes. Then the vessel was sealed and heated at 140 °C for 7 days. Colorless or pale-yellow octahedral crystals (yield: 70 mg, ca. 41% base on *n*-butylSnCl<sub>3</sub>) with pure phase were obtained by filtration after being washed with DMF and acetone for several times. Experimental EA date: C 23.78%, H 3.85%, N 6.19%, S 19.83%; calculated EA date: C 23.75%, H 3.68%, N 7.92%, S 18.13%. Experimental ICP data: Sn 42.12%; calculated ICP date: Sn: 41.95%. IR:  $\nu$  (cm<sup>-1</sup>) = 3430(w), 3197(w), 3108(w), 2955(m), 2874(w), 2778(w), 2041(w), 1674(s), 1592(w), 1454(w), 1419(w), 1377(w), 1307(m), 1207(w), 1124(w), 1066(w), 575(m), 459(w).

**Synthesis of T3-SnOSe-MTN.** *n*-butylSnCl<sub>3</sub> (0.1 mL), SeO<sub>2</sub> (2 mmol), DBA (0.8 mL), [BMMIm]Cl (4 mmol), DMSO (0.2 mL), were mixed in a 23-mL Teflon-lined stainless autoclave and stirred for 20 minutes. Then the vessel was sealed and heated at 120 °C for 15 days. Orange octahedral crystals (yield: 17 mg) with pure phase were obtained by filtration after being washed with ethanol for several times. Experimental EA date: C 16.77%, H 2.86%, N 3.55%, S 0.76%; calculated EA date: C: 16.01%, H: 2.96%, N: 4.87%; S: 0.93%; Experimental ICP date: Sn 31.12%, Se 36.21%; calculated ICP date: Sn: 34.41%, Se: 36.62%. IR:  $\nu$  (cm<sup>-1</sup>) = 3122(w), 2913(m), 2860(m), 1575(w), 1525(w), 1448(m), 1372(w), 1237(w), 1184(w), 1128(w), 1035(w), 950(w), 856(w), 726(m), 649(m), 548(s).

### Section S3: Crystallographic Data

**Table S1** Lattice parameters of T3-SnOX-MTN (X = S/Se) by SCXRD

Compound Name	T3-SnOS-MTN	T3-SnOSe-MTN
$a/\text{\AA}$	74.1412(3)	76.479(4)
$b/\text{\AA}$	74.1412(3)	76.676(4)
$c/\text{\AA}$	74.1412(3)	76.396(4)
$\alpha/^\circ$	90	89.848(5)
$\beta/^\circ$	90	89.829(5)
$\gamma/^\circ$	90	89.763(5)
Volume / $\text{\AA}^3$	407548 (3)	447985 (40)

**Table S2** Crystallographic data of T3-SnOS-MTN

Empirical Formula	H <sub>8</sub> O <sub>8</sub> S <sub>16</sub> Sn <sub>10</sub>
Formula Weight	1836.217
Temperature/K	77
Crystal System	cubic
Space Group	<i>Fd-3m</i>
<i>a</i> /Å	74.1412(3)
<i>b</i> /Å	74.1412(3)
<i>c</i> /Å	74.1412(3)
$\alpha$ /°	90
$\beta$ /°	90
$\gamma$ /°	90
Volume/Å <sup>3</sup>	407548(6)
<i>Z</i>	136
$\rho_{\text{calc}}$ /g cm <sup>-3</sup>	1.013
$\mu$ /mm <sup>-1</sup>	12.687
F(000)	113770.9
Crystal Size/mm <sup>3</sup>	0.4 × 0.35 × 0.35
Radiation	GaK $\alpha$ ( $\lambda$ = 1.3405)
2 $\theta$ Range for Data Collection/°	6.22 to 79.96
Index Ranges	-82 ≤ <i>h</i> ≤ 38, -90 ≤ <i>k</i> ≤ 53, -48 ≤ <i>l</i> ≤ 72
Reflections Collected	111223
Independent Reflections	8546 [ <i>R</i> <sub>int</sub> = 0.0309, <i>R</i> <sub>sigma</sub> = 0.0234]
Data/Restraints/Parameters	8546/0/266
Goodness-of-Fit on F <sup>2</sup>	0.925
Final <i>R</i> Indexes [ <i>I</i> ≥ 2 $\sigma$ ( <i>I</i> )]	<i>R</i> <sub>1</sub> = 0.0556, <i>wR</i> <sub>2</sub> = 0.1903
Final <i>R</i> Indexes [all data]	<i>R</i> <sub>1</sub> = 0.0645, <i>wR</i> <sub>2</sub> = 0.2022
Largest Diff. Peak/Hole / e Å <sup>-3</sup>	0.74/-0.72

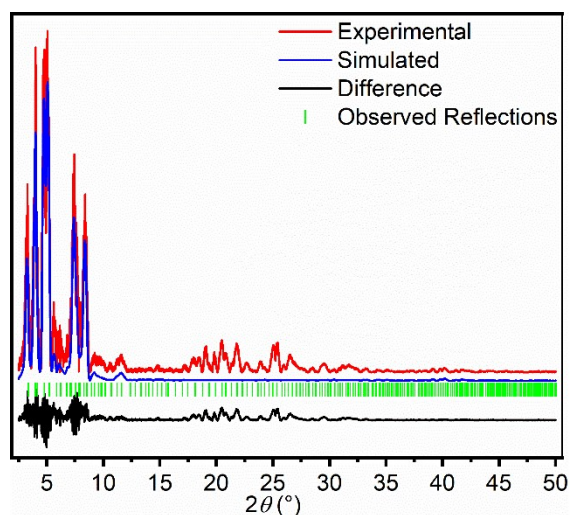


**Fig. S1** Experimental and simulated PXRD patterns of T3-SnOSe-MTN after Pawley refinement. The reflection positions are represented by the green bars.

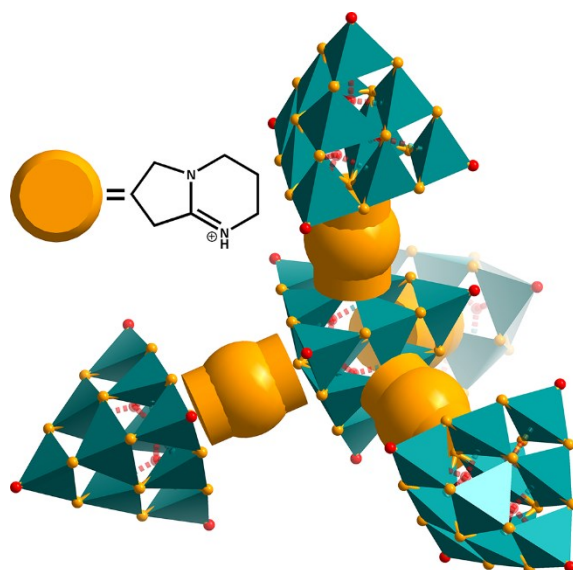


**Fig. S2** The linkage mode between oxido-filled-T3  $\{\text{Sn}_{10}\text{O}_8\text{S}_{16}\}$  clusters, each of which connects to four neighbors via the Coulombic interactions with the protonated organic amine templates of  $\text{H}^+\text{DBN}$ .



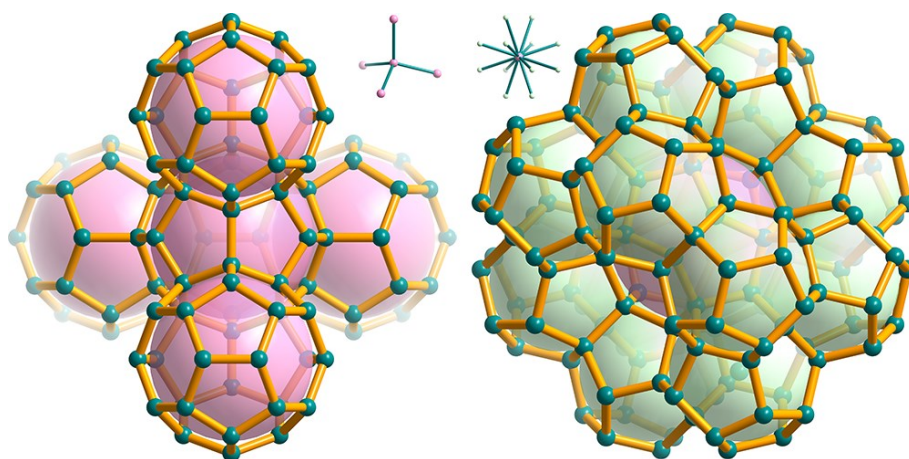


**Fig. S3** Each cage-A ( $6^4 5^{12}$ ) surrounded by 4 cage-A ( $6^4 5^{12}$ ) and 12 cage-B ( $5^{12}$ ) in T3-SnOS-MTN.

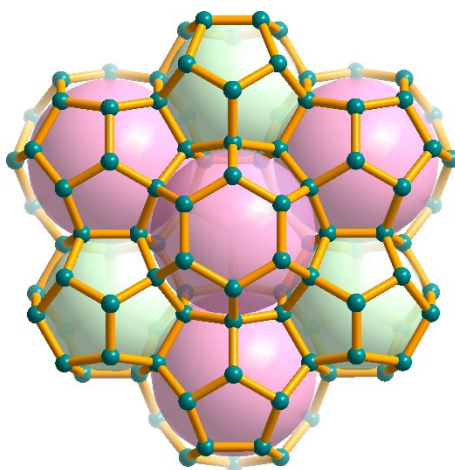


**Fig. S4** The  $\{\text{Sn}_{10}\text{O}_8\text{S}_{16}\}^{8-}$  anions are scattered in 3D space in an MTN zeotype in which each cluster is treated as a node.

#### Section S4: Fourier-Transform Infrared (FT-IR) Spectroscopy and Thermogravimetric Analysis (TGA)

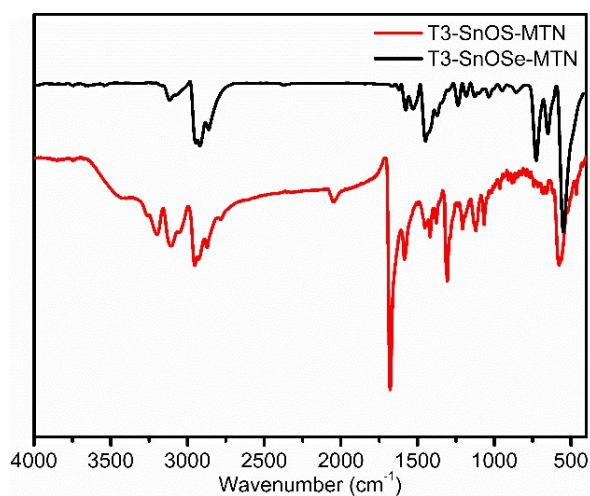


**Fig. S5** The FT-IR spectra of samples of T3-SnOX-MTN (X = S/Se).

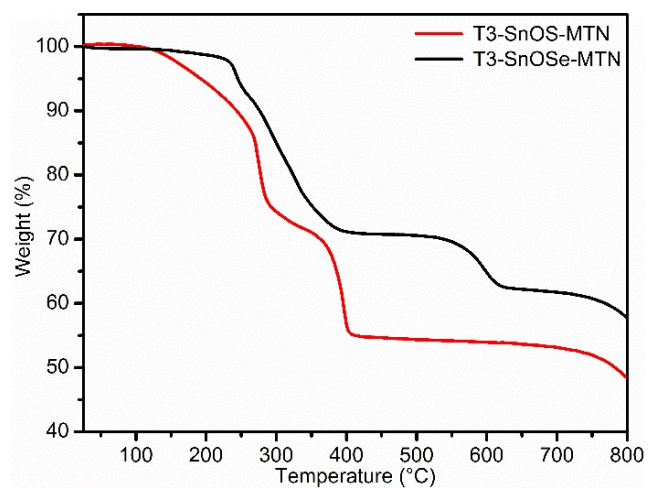


**Fig. S6** The TGA curves of samples of T3-SnOX-MTN (X = S/Se).

## Section S5: Scanning Electron Microscopy (SEM) and X-ray Energy

### Dispersive Spectroscopy (EDS)

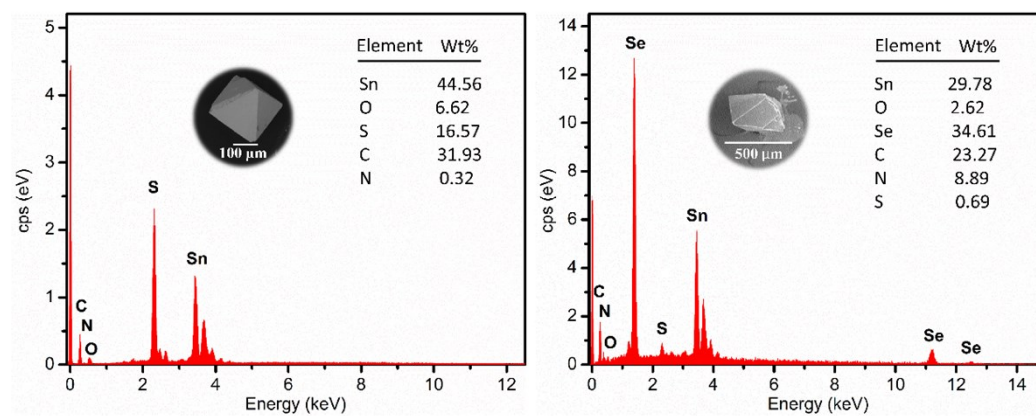


**Fig. S7** The SEM images and EDS spectra of T3-SnOS-MTN (left) and T3-SnOSe-MTN (right). For T3-SnOSe-MTN, trace amount of S could be attributed to the presence of guest molecule of DMSO.

## Section S6: Electrospray Ionization Mass Spectrometry (ESI–MS)

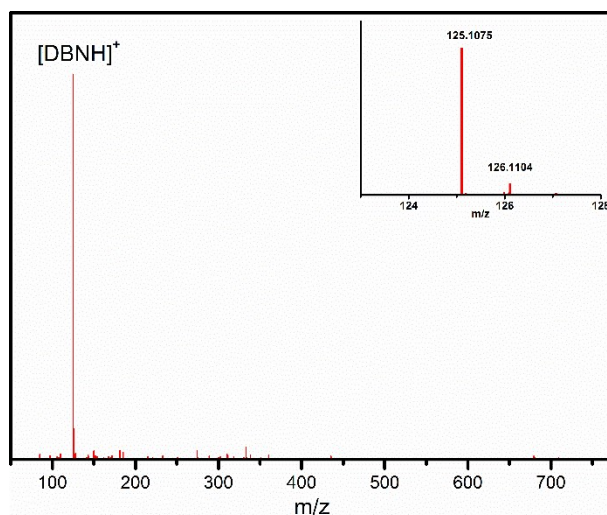


**Fig. S8** The positive-mode ESI-MS spectrum of T3-SnOS-MTN in  $\text{CH}_3\text{CN}$ . The main peak at 125.1075 can be assignable to species of  $\text{H}^+\text{DBA}$  (i.e.,  $[\text{C}_7\text{H}_{13}\text{N}_2]^+$ ).

## Section S7: Gas Sorption (BET)

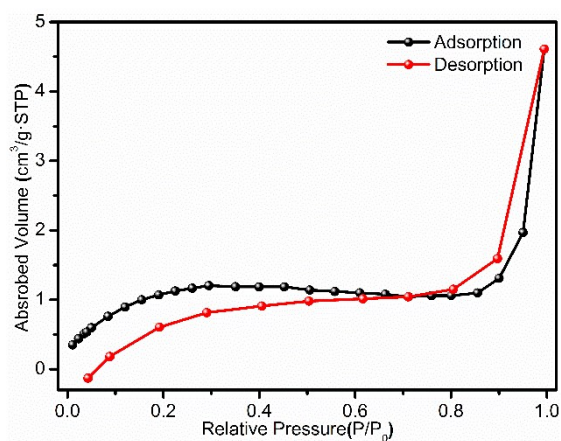


**Fig. S9** The N<sub>2</sub> adsorption-desorption isotherms of T3-SnOS-MTN at 77 K.

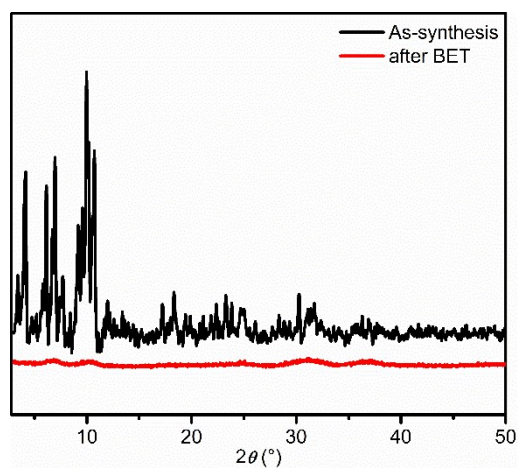


**Fig. S10** The PXRD patterns of T3-SnOS-MTN as-synthesis and after the BET testing.

## Section S8: Photoluminescence (PL)

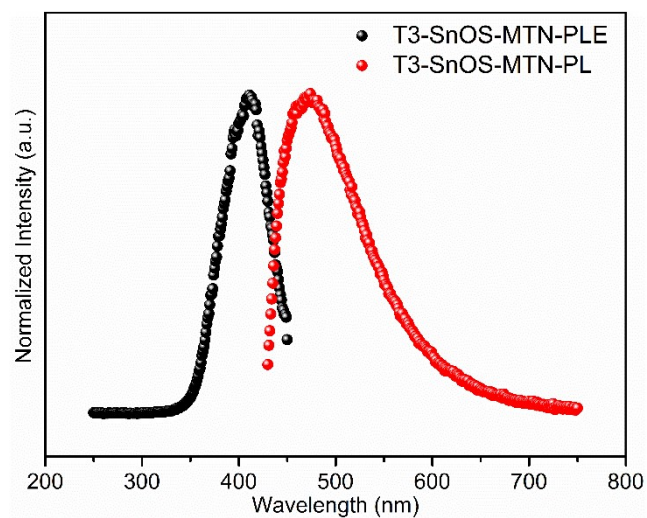


**Fig. S11** The photoluminescence spectra of T3-SnOS-MTN.

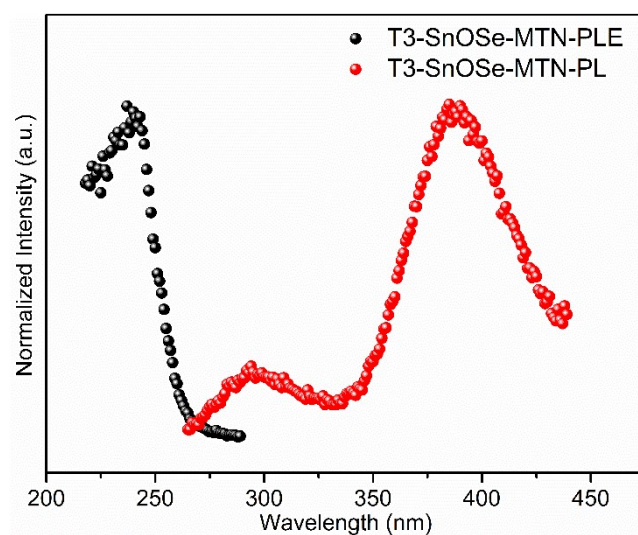


**Fig. S12** The photoluminescence spectra of T3-SnOSe-MTN.



## Section S9: Proton Conduction

**Impedance Analysis.** The sample was put into a home-made mold with a radius of 0.2 cm to get circular pellet, whose thickness was measured by a Vernier caliper. Then silver colloid were smeared on both sides of the pellet for fixing copper wires. The proton conductive capacities were performed on a Zahner (IM6) electrochemical impedance spectrometer, over sweeping from 0.1 Hz to 10 MHz, under varying relative humidity. The proton conductivity was calculated by using the following equation

$$\sigma = l/SR$$

where  $\sigma$  is the conductivity ( $S\text{ cm}^{-1}$ ).  $l$  is the thickness (cm) of the pellet,  $S$  is the cross-sectional area ( $\text{cm}^2$ ) of the pellet,  $R$  is the bulk resistance ( $\Omega$ ). The activation energy ( $E_a$ ) was calculated from the following equation

$$\ln \sigma T = \ln \sigma_0 - E_a/KT$$

where  $\sigma$  is the conductivity ( $S\text{ cm}^{-1}$ ),  $K$  is the Boltzmann constant ( $\text{eV/K}$ ) and  $T$  is the temperature (K)

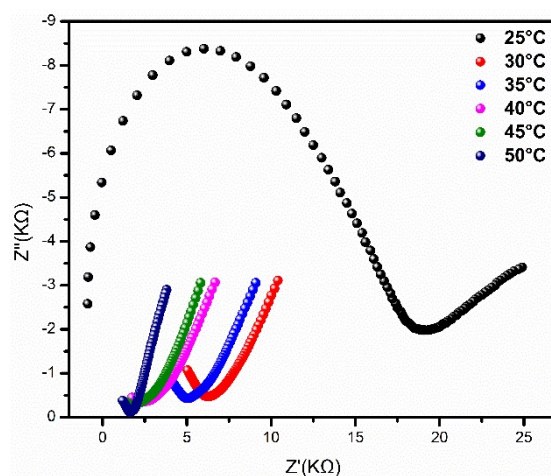


**Fig. S13** Nyquist plots of the pelleted sample of T3-SnOS-MTN at different temperatures under 98% RH.

## Section S10: References

- 1 (a) O. V. Dolomanov, L. J. Bourhis, R. J. Gildea, J. A. K. Howard and H. Puschmann, *J. Appl. Cryst.*, 2009, **42**, 339-341; (b) G. Sheldrick, *Acta Cryst.*, 2015, **C71**, 3-8; (c) L. J. Bourhis, O. V. Dolomanov, R. J. Gildea, J. A. K. Howard and H. Puschmann, *Acta Cryst.*, 2015, **A71**, 59-75.
- 2 P. van der Sluis and A. L. Spek, *Acta Cryst.*, 1990, **A46**, 194-201.